Supplementary Information for

The long noncoding RNA *SChLAP1* promotes aggressive prostate cancer and antagonizes the SWI/SNF complex

John R. Prensner[1,10], Matthew K. Iyer[1,2,10], Anirban Sahu[1,10], Irfan A. Asangani[1], Qi Cao[1], Lalit Patel[1,3], Ismael A. Vergara[4], Elai Davicioni[4], Nicholas Erho[4], Mercedeh Ghadessi[4], Robert B. Jenkins[5], Timothy J. Triche[4], Rohit Malik[1], Rachel Bedenis[3], Natalie McGregor[3], Teng Ma[6], Wei Chen[6], Sumin Han[6], Xiaojun Jing[1], Xuhong Cao[1], Xiaoju Wang[1], Benjamin Chandler[1], Wei Yan[1], Javed Siddiqui[1], Lakshmi P. Kunju[1,7,8], Saravana M. Dhanasekaran[1,7], Kenneth J. Pienta[1,3], Felix Y. Feng[1,6,8], Arul M. Chinnaiyan[1,2,7,8,9]

[1]Michigan Center for Translational Pathology, University of Michigan, Ann Arbor, Michigan USA.
[2]Department of Computational Medicine and Bioinformatics, Ann Arbor, Michigan USA.
[3]Department of Internal Medicine, University of Michigan, Ann Arbor, Michigan USA.
[4]GenomeDx Biosciences Inc., Vancouver, British Columbia, Canada.
[5]Department of Laboratory Medicine and Pathology, Mayo Clinic, Rochester, Minnesota USA.
[6]Department of Radiation Oncology, University of Michigan, Ann Arbor, Michigan USA.
[7]Department of Pathology, University of Michigan, Ann Arbor, Michigan USA.
[8]Comprehensive Cancer Center, University of Michigan, Ann Arbor, Michigan USA.
[9]Howard Hughes Medical Institute, University of Michigan, Ann Arbor, Michigan USA.
[10]These authors contributed equally.

Address correspondence to:
Arul M. Chinnaiyan, M.D. Ph.D.
Investigator, Howard Hughes Medical Institute
Comprehensive Cancer Center
University of Michigan Medical School
1400 E. Medical Center Dr. 5316 CCGC 5940
Ann Arbor, MI 48109-5940
arul@med.umich.edu

This PDF file includes:

Supplementary Note
Supplementary Figures 1-14

Other Supplementary Materials for this manuscript includes the following:

Supplementary Tables 1-8 as zipped archive: *Supplementary Tables*

Supplementary Note

Development of a *SChLAP1* ISH assay

To optimize an ISH assay for *SChLAP1*, we first employed a panel of samples previously analyzed for *SChLAP1* expression by qPCR. For this, we validated our ISH assay on 9 FFPE samples (3 PCAs positive for *SChLAP1*, 3 PCAs negative for *SChLAP1*, and 3 benign tissues) with matched qPCR data, and we observed high concordance between our qPCR and ISH results (**Supplementary Fig. 4a**). Following this confirmation of our method, we used ISH to analyze a tissue microarray (TMA) repressing 22 metastatic PCAs and 8 localized PCAs (**Supplementary Fig. 4b**). These data were used to generate the images used in **Fig. 1**.

Development of prostate cancer gene signatures from RNA-Seq data

To analyze the clinical significance of *SChLAP1*, we evaluated its association to aggressive gene signatures. We used publically available data from the Oncomine database to extract prostate cancer clinical concepts. Next, we evaluated the statistical association between each dataset in our clinical concept compendium with the gene signatures derived from correlation analysis. For this analysis, we also included signatures from our RNA-Seq cohort delineating localized cancer vs. benign tissues, high grade localized prostate cancer (Gleason ≥8 vs. Gleason 6), and metastatic vs. primary tumors (**Supplementary Fig. 5** and **Supplementary Table 3**). Here, we used statistical modeling to identify genes that distinguish these sample sets from each other. To evaluate the overlap of the *SChLAP1* gene signature with these clinical gene signatures, we computed odds ratios, p-values, and q-values for each comparison (one-sided Fisher's exact test, **Methods**).

SChLAP1 as a prognostic biomarker

Our analysis of *SChLAP1* utilizes a clinical cohort of patients with high-risk features, such as highly elevated PSA levels. Thus, our data suggest that *SChLAP1* expression retains its prognostic utility for defining a subgroup of patients more likely to experience BCR, CP, and PCSM even in high-risk patients, where most individuals experienced disease recurrence within ten years post-prostatectomy. We further noted that *SChLAP1* expression is a particularly strong prognostic indicator for CP and PCSM, which is important, as it is known that patients who develop BCR do not necessarily progress further to lethal or clinically significant recurrent disease: that is, many patients who experience BCR nevertheless die with prostate cancer but not from it[1,2]. As such, CP and PCSM represent more stringent criteria to define aggressive prostate cancer. Thus, our data suggest that *SChLAP1* is a powerful biomarker of lethal disease.

Note on human research samples

We employed two sets of prostate cancer samples for this study. For the University of Michigan cohort, patients provided informed consent and enabled biomedical research using their tissue samples according to an institutional review board-approved protocol as detailed in the Methods section. Metastatic prostate cancer samples were obtained through the Rapid Autopsy Program operated through the University of Michigan Prostate Cancer Specialized Program Of Research Excellence (S.P.O.R.E.).

For the Mayo Clinic cohort, eligible patients provided informed consent according to an institutional review board-approved protocol as detailed in the Methods section. Briefly, men with high risk disease were selected for the current student as defined by cancer histology, PSA values, and local invasion of adjacent structures by the cancer.

a

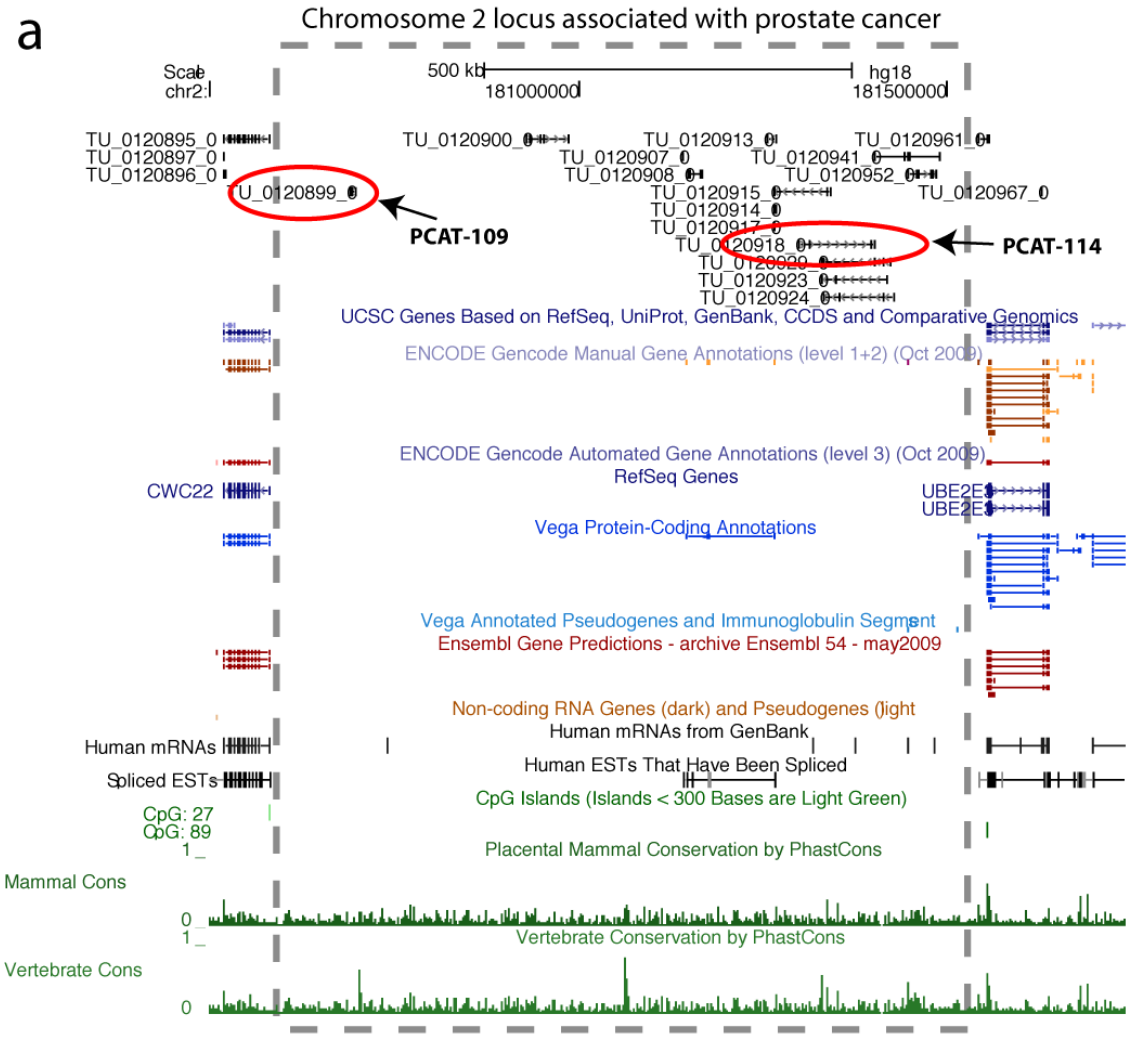

b

Gene	*Score*	*Location*	*Freq. (%)*	*RPKM (min, max)*	*Cell lines > 2RPKM?*	*In mets?*
PCAT-109	123.542	chr2:180689090-180696402	17.74	0, 93.6	No	Yes
PCAT-114	112.710	chr2:181297540-181400892	24.19	0, 91.2	Yes	Yes
PCAT-113	68.357	chr1:20685471-20686432	9.68	0, 1374.2	Yes	Yes
PCAT-115	60.918	chr10:42652247-42653596	27.42	0, 64.8	No	No
PCAT-118	55.844	chr2:180926864-180985967	14.52	0, 66.7	No	Yes
PCAT-29	53.883	chr15:67764259-67801825	30.65	0, 88	Yes	Yes
TU_0102399	46.665	chr9:35759438-35761676	27.42	0, 178.7	Yes	Yes
PCAT-68	44.507	chr13:33918267-33935946	32.26	0, 14.2	No	Yes
PCAT-1	41.420	chr8:128138926-128140075	30.65	0, 37.7	No	Yes
TU_0108439	39.132	chr15:19293567-19296333	29.03	0, 26.8	No	Yes
TU_0030420	38.715	chrX:112642982-112685485	14.52	0, 62	No	Yes
TU_0098644	36.779	chr8:81204784-81207034	33.87	0, 34.9	No	Yes
TU_0050712	34.231	chr4:170217424-170228463	12.90	0, 64.6	Yes	Yes
TU_0001173	31.823	chr6:26385234-26386052	35.48	0, 70.3	Yes	Yes
PCAT-76	31.010	chr20:55779532-55780817	17.74	0, 25.7	Yes	Yes

Supplementary Figure 1: Nomination of *SChLAP1*. **(a)** A gene desert on chr2q31 between *CWC22* and *UBE2E3* contains multiple transcripts that are upregulated in prostate cancer, including the predicted outliers *PCAT-109* and *PCAT-114*. These transcripts are unannotated in major gene annotation databases. (**b**) A comparison of lncRNA outliers nominated by COPA, including their location, frequency in clinical samples, their expression in tissues and cell lines, and whether they occur in metastatic prostate samples.

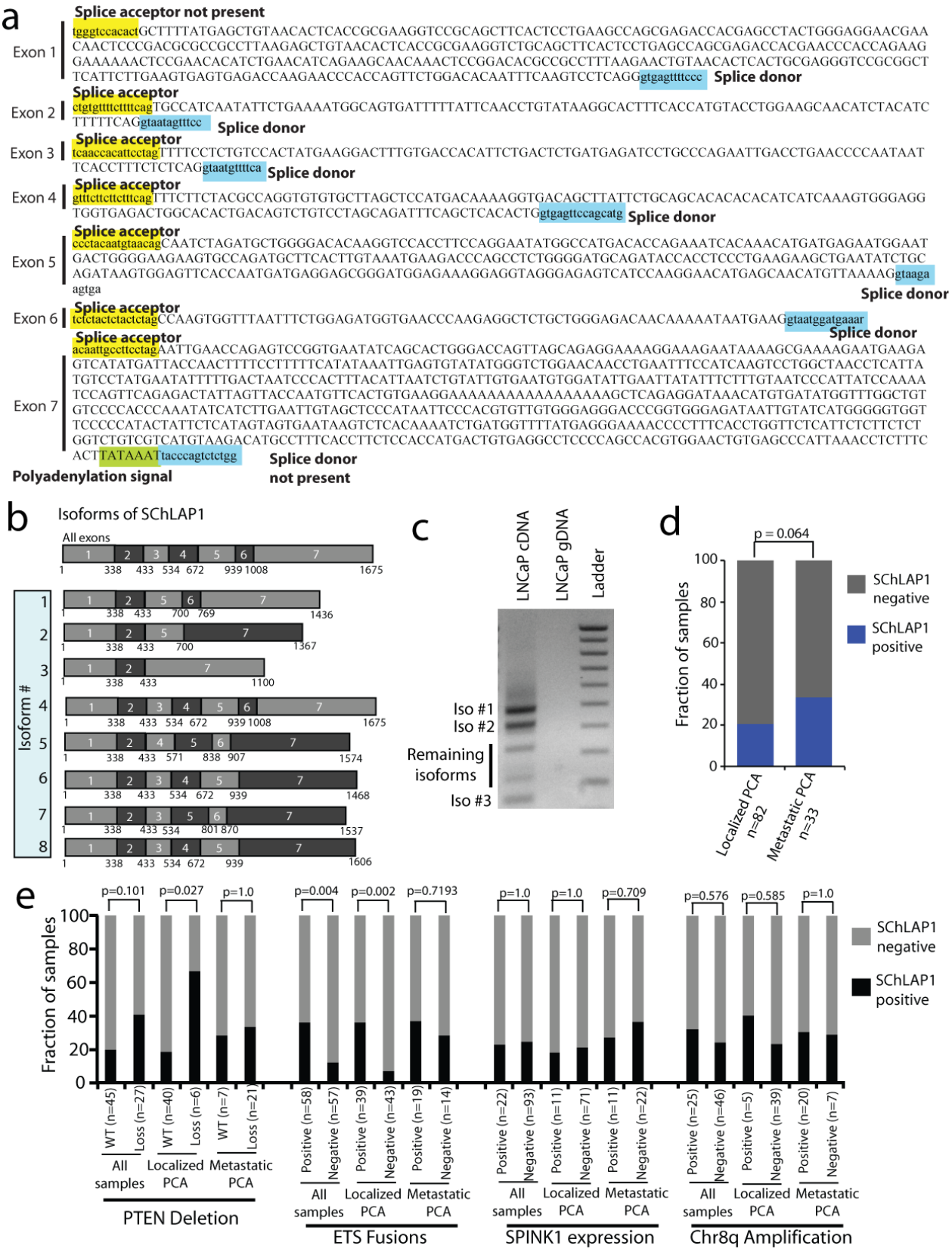
a
Splice acceptor not present
Exon 1
tgggtccacactGCTTTTATGAGCTGTAACACTCACCGCGAAGGTCCGCAGCTTCACTCCTGAAGCCAGCGAGACCACGAGCCTACTGGGAGGAACGAA
CAACTCCCGACGCGCCGCCTTAAGAGCTGTAACACTCACCGCGAAGGTCTGCAGCTTCACTCCTGAGCCAGCGAGACCACGAACCCACCAGAAG
GAAAAAACTCCGAACACATCTGAACATCAGAAGCAACAAACTCCGGACACGCCGCCTTTAAGAACTGTAACACTCACTGCGAGGGTCCGCGGCT
TCATTCTTGAAGTGAGTGAGACCAAGAACCCACCAGTTCTGGACACAATTTCAAGTCCTCAGGgtgagttttccc
Splice donor
Splice acceptor
Exon 2
ctgtgttttcttttcagTGCCATCAATATTCTGAAAATGGCAGTGATTTTTATTCAACCTGTATAAGGCACTTTCACCATGTACCTGGAAGCAACATCTACATC
TTTTTCAGgtaatagtttcc
Splice donor
Splice acceptor
Exon 3
tcaaccacattcctagTTTTCCTCTGTCCACTATGAAGGACTTTGTGACCACATTCTGACTCTGATGAGATCCTGCCCAGAATTGACCTGAACCCCAATAAT
TCACCTTTCTCTCAGgtaatgttttca
Splice donor
Splice acceptor
Exon 4
gtttcttcttctttcagTTTCTTCTACGCCAGGTGTGTGCTTAGCTCCATGACAAAAGGTGACAGCTTATTCTGCAGCACACACACATCATCAAAGTGGGAGG
TGGTGAGACTGGCACACTGACAGTCTGTCCTAGCAGATTTCAGCTCACACTGgtgagttccagcatg
Splice donor
Splice acceptor
Exon 5
ccctacaatgtaacagCAATCTAGATGCTGGGGACACAAGGTCCACCTTCCAGGAATATGGCCATGACACCAGAAATCACAAACATGATGAGAATGGAAT
GACTGGGGAAGAAGTGCCAGATGCTTCACTTGTAAATGAAGACCCAGCCTCTGGGGATGCAGATACCACCTCCCTGAAGAAGCTGAATATCTGC
AGATAAGTGGAGTTCACCAATGATGAGGAGCGGGATGGAGAAAGGAGGTAGGGAGAGTCATCCAAGGAACATGAGCAACATGTTAAAAGgtaaga
agtga
Splice donor
Splice acceptor
Exon 6
tctctactctactctagCCAAGTGGTTTAATTTCTGGAGATGGTGAACCCAAGAGGCTCTGCTGGGAGACAACAAAAATAATGAAGgtaatggatgaaar
Splice donor
Splice acceptor
Exon 7
acaattgccttcctagAATTGAACCAGAGTCCGGTGAATATCAGCACTGGGACCAGTTAGCAGAGGAAAAGGAAAGAATAAAAGCGAAAAGAATGAAGA
GTCATATGATTACCAACTTTTCCTTTTTCATATAAATTGAGTGTATATGGGTCTGGAACAACCTGAATTTCCATCAAGTCCTGGCTAACCTCATTA
TGTCCTATGAATATTTTTGACTAATCCCACTTTACATTAATCTGTATTGTGAATGTGGATATTGAATTATATTTCTTTGTAATCCCATTATCCAAAA
TCCAGTTCAGAGACTATTAGTTACCAATGTTCACTGTGAAGGAAAAAAAAAAAAAAAAAAGCTCAGAGGATAAACATGTGATATGGTTTGGCTGT
GTCCCCACCCAAATATCATCTTGAATTGTAGCTCCCATAATTCCCACGTGTTGTGGGAGGGACCCGGTGGGAGATAATTGTATCATGGGGGTGGT
TCCCCCATACTATTCTCATAGTAGTGAATAAGTCTCACAAAATCTGATGGTTTTATGAGGGAAAACCCCTTTCACCTGGTTCTCATTCTCTTCTCT
GGTCTGTCGTCATGTAAGACATGCCTTTCACCTTCTCCACCATGACTGTGAGGCCTCCCCAGCCACGTGGAACTGTGAGCCCATTAAACCTCTTTC
ACTTATAAATtacccagtctctgg
Splice donor not present
Polyadenylation signal
b
Isoforms of SChLAP1
All exons
1 2 3 4 5 6 7
1 338 433 534 672 939 1008 1675
Isoform #
1 1 2 5 6 7 1436
2 1 2 5 7 1367
3 1 2 7 1100
4 1 2 3 4 5 6 7 1675
5 1 2 4 5 6 7 1574
6 1 2 3 4 5 7 1468
7 1 2 3 5 6 7 1537
8 1 2 3 4 5 7 1606
c
LNCaP cDNA
LNCaP gDNA
Ladder
Iso #1
Iso #2
Remaining isoforms
Iso #3
d
p = 0.064
Fraction of samples
100
80
60
40
20
0
SChLAP1 negative
SChLAP1 positive
Localized PCA n=82
Metastatic PCA n=33
e
p=0.101 p=0.027 p=1.0 p=0.004 p=0.002 p=0.7193 p=1.0 p=1.0 p=0.709 p=0.576 p=0.585 p=1.0
Fraction of samples
100
80
60
40
20
0
SChLAP1 negative
SChLAP1 positive
WT (n=45) Loss (n=27) WT (n=40) Loss (n=6) WT (n=7) Loss (n=21)
All samples
Localized PCA
Metastatic PCA
PTEN Deletion
Positive (n=58) Negative (n=57) Positive (n=39) Negative (n=43) Positive (n=19) Negative (n=14)
ETS Fusions
Positive (n=22) Negative (n=93) Positive (n=11) Negative (n=71) Positive (n=11) Negative (n=22)
SPINK1 expression
Positive (n=25) Negative (n=46) Positive (n=5) Negative (n=39) Positive (n=20) Negative (n=7)
Chr8q Amplification

Supplementary Figure 2: Characterization of *SChLAP1* and its expression. (a) The sequences of the seven exons found in the *SChLAP1* gene are detailed here, indicating the presence of splice donor and splice acceptor sites. Interestingly, the promoter for *SChLAP1* lacks a CpG island but instead has remnants of a long terminal repeat from an ancestral retrovirus. Nucleotides comprising the *SChLAP1* gene are capitalized, whereas genomic non-*SChLAP1* basepairs are in lower case font. (**b**) A schematic summarizing the observed *SChLAP1* isoforms. A total of 8 isoforms were observed, with isoform #1 and isoform #2 accounting for >90% of transcripts. **(c)** Abundance of SChLAP1 isoforms by RT-PCR in LNCaP cells. Isoforms 1, 2, and 3 were cloned for experimental use. **(d)** Prevalence of SChLAP1 expression in localized prostate cancer tissues and metastatic prostate cancer tissues. P value was determined by one-sided Fisher's exact test. **(e)** SChLAP1 prevalence in molecular subtypes of prostate cancer. Prostate cancer samples were stratified by available data for SPINK1 expression (determined by qPCR), PTEN deletion or Chr8q amplification (determined by array CGH or ETS fusions (ERG and ETV1 determined by break-apart FISH). Data have been previously published in[3-5]. SChLAP1 demonstrates a significant association with ETS fusion status and PTEN deletion status in localized but not metastatic prostate cancer. SChLAP1 demonstrates no association with Chr8q amplification of SPINK1 expression. P values determined by a two-sided Fisher's exact test.

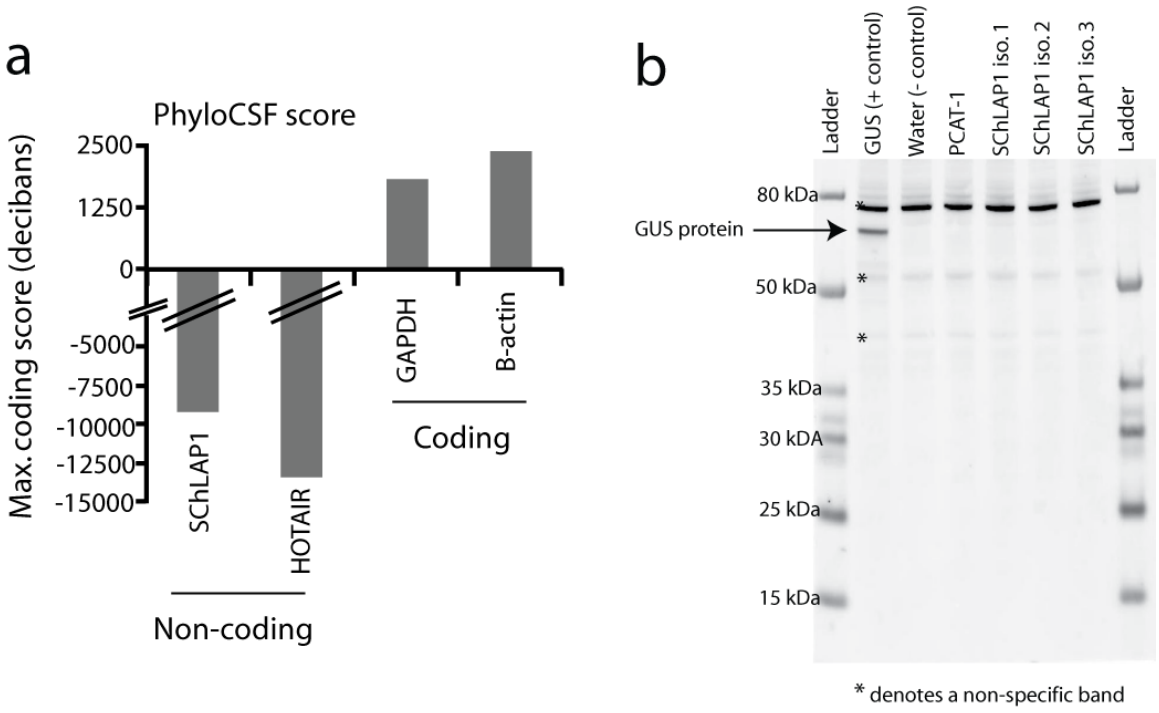

Supplementary Figure 3: *SChLAP1* is a non-coding gene.

(a) Analysis of the coding potential for the *SChLAP1* sequence across 29 mammals in all 3 reading frames using PhyloCSF. *HOTAIR* serves as a control non-coding gene. *GAPDH* and *B-actin* serve as control coding genes. Scores above 0 suggest coding potential whereas scores below 0 suggest no coding potential. **(b)** *In vitro* translation assays for *SChLAP1*. Three isoforms of *SChLAP1* were cloned and tested for protein-coding capacity using an *in vitro* translation assay. GUS is used as a positive control. *PCAT-1* and water serve as negative controls. Non-specific bands are indicated with an asterisk. *SChLAP1* isoforms do not generate a protein in this assay.

a

Tissue	SChLAP1 qPCR	SChLAP1 ISH
Benign_1	0.373	0
Benign_2	0.761	0
Benign_3	2.540	1
PCA_1	52.182	3
PCA_2	0.509	1
PCA_3	0.267	1
PCA_4	117.353	4
PCA_5	44.242	4
PCA_6	0.411	0

b

		SChLAP1 score				
Type	N	4	3	2	1	0
PCA	8	1	0	3	0	4
MET	22	6	2	2	0	12

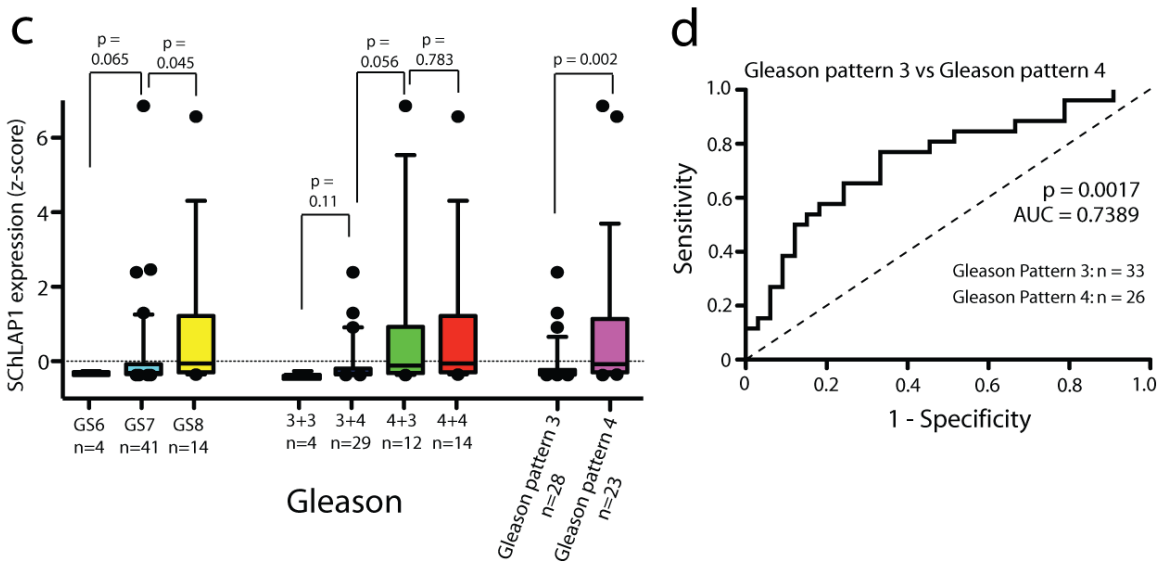

Supplementary Figure 4: *SChLAP1* expression is associated with cancer histology.

(a) Concordance between *SChLAP1* in situ hybridization data and *SChLAP1* qPCR data for 9 tissue samples. A cut-off of 5 was used to determine positivity of *SChLAP1* by qPCR and a cut-off of 3 was used to determine *SChLAP1*-positive samples by ISH. **(b)** *In situ* hybridization data for *SChLAP1* a panel of 8 localized prostate cancers and 22 metastatic prostate cancers. **(c)** Boxplot analysis of SChLAP1 expression in Gleason score. *Left*, SChLAP1 expression in Gleason 6, 7 or 8 samples. *Middle*, SChLAP1 expression when Gleason 7 is subdivided into 3+4 and 4+3 histology. *Right*, SChLAP1 expression in Gleason pattern 3 cancers (Gleason 3+3 and 3+4) compared to Gleason pattern 4 cancers (Gleason 4+3 and 4+4). P values determined by Mann-Whitney U test. **(d)** ROC analysis demonstrating the ability for SChLAP1 to discriminate between Gleason pattern 3 and Gleason pattern 4 prostate cancer.

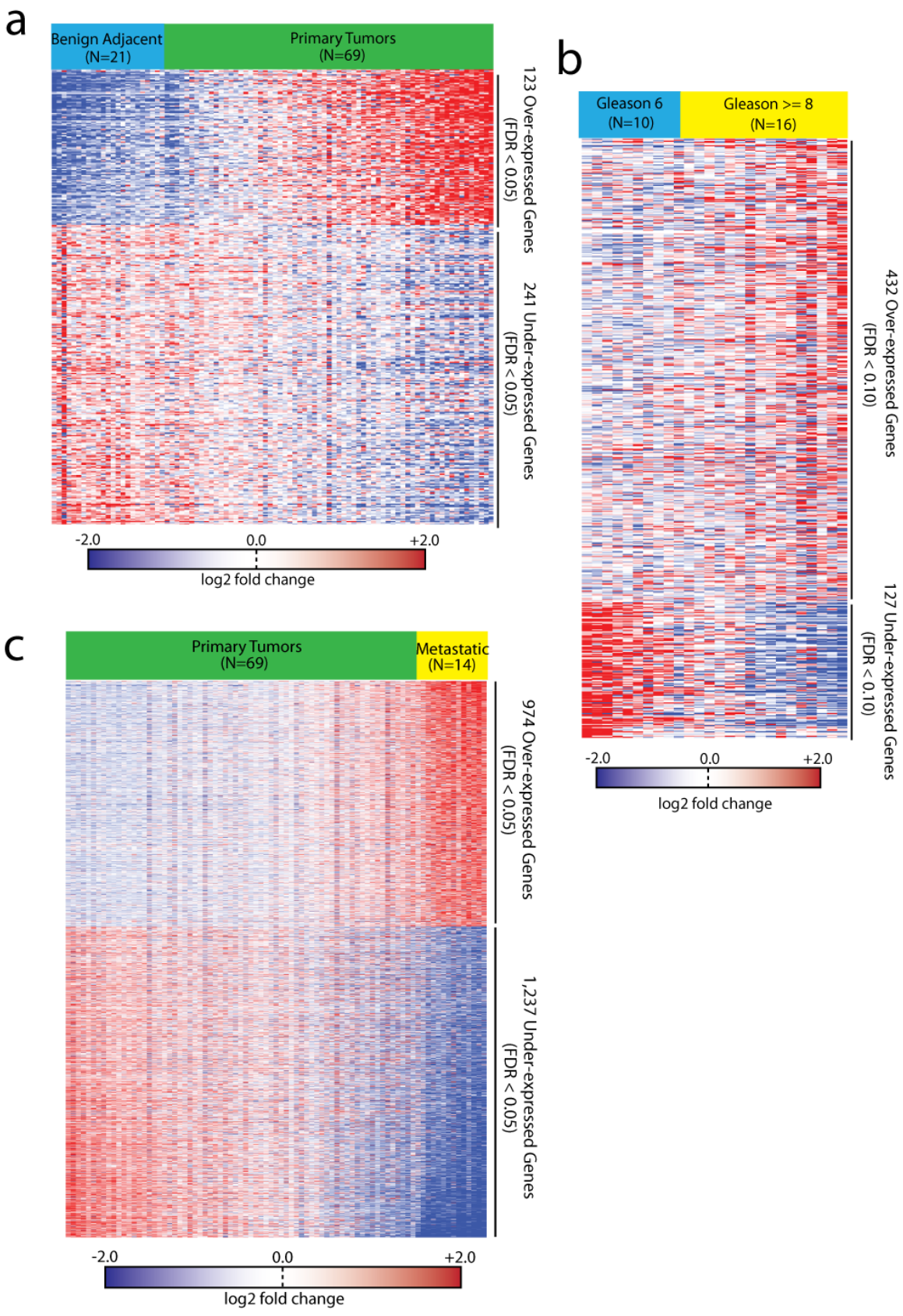
a
Benign Adjacent (N=21)
Primary Tumors (N=69)
123 Over-expressed Genes (FDR < 0.05)
241 Under-expressed Genes (FDR < 0.05)
-2.0
0.0
+2.0
log2 fold change
b
Gleason 6 (N=10)
Gleason >= 8 (N=16)
432 Over-expressed Genes (FDR < 0.10)
127 Under-expressed Genes (FDR < 0.10)
-2.0
0.0
+2.0
log2 fold change
c
Primary Tumors (N=69)
Metastatic (N=14)
974 Over-expressed Genes (FDR < 0.05)
1,237 Under-expressed Genes (FDR < 0.05)
-2.0
0.0
+2.0
log2 fold change

Supplementary Figure 5: Generation of prostate cancer gene signatures from RNA-Seq data.

(a) Heatmap analysis defines a gene expression signature from RNA-seq data distinguishing benign prostate tissues and localized prostate cancer tissues. **(b)** Heatmap analysis defines a gene expression signature from RNA-seq data distinguishing low grade from high grade localized prostate cancer tissues. **(c)** Heatmap analysis defines a gene expression signature from RNA-seq data distinguishing localized prostate cancer tissues from metastatic cancers.

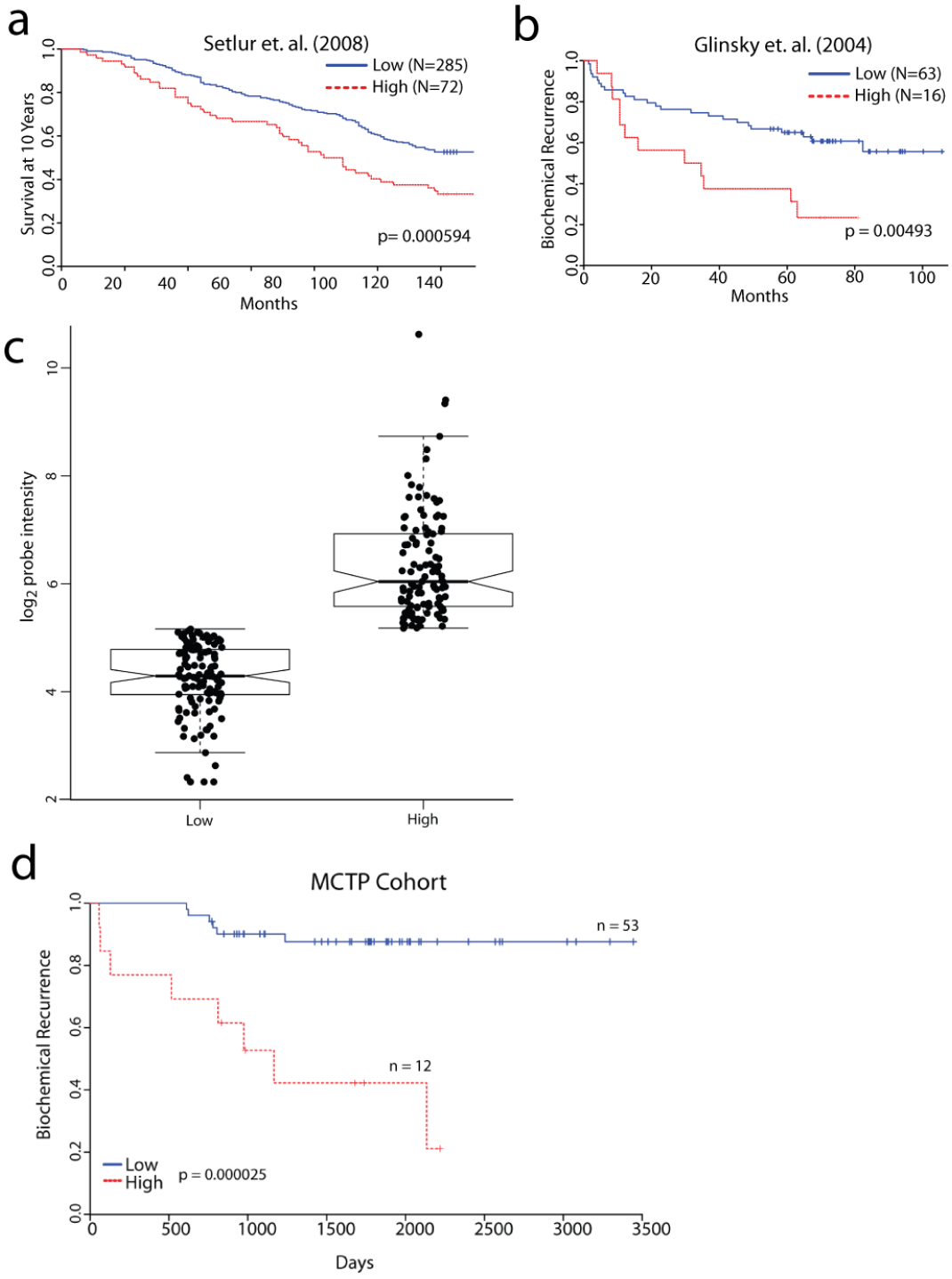

Supplementary Figure 6: *SChLAP1* expression stratifies prostate cancer patient outcomes.

(a) Kaplan-Meier analysis of prostate cancer outcomes. Patients were stratified according to their *SChLAP1* signature score. Signature scores at or above the 80th percentile were

deemed ‘High’, and the rest ‘Low’. Statistical significance was determined by the log rank test. Analysis of the 10-year overall survival probability for prostate cancer patients from the Setlur *et al.* study[6]. **(b)** As in **(a)**, Analysis of the biochemical recurrence probability for prostate cancer patients from the Glinksy *et al.* study[7]. **(c)** *SChLAP1* expression in the Mayo Clinic cohort. Prostate cancer tissue samples were analyzed for gene expression using Affymetrix Human Exon 1.0 ST GeneChips and probe 2518129 was used as representative of the *SChLAP1* gene. PAM unsupervised analysis (see **Methods**) of the expression data clustered samples into *SChLAP1*-low and *SChLAP1*-high expression cohorts. Notches indicate 95% confidence intervals for each group. **(d)** *SChLAP1* predicts for biochemical recurrence in the University of Michigan cohort. *SChLAP1* expression was measured using qPCR on a cohort of fresh-frozen prostate cancer tissue samples from radical prostatectomy patients for whom follow-up for biochemical recurrence was available. Statistical significance was determined by the log-rank test.

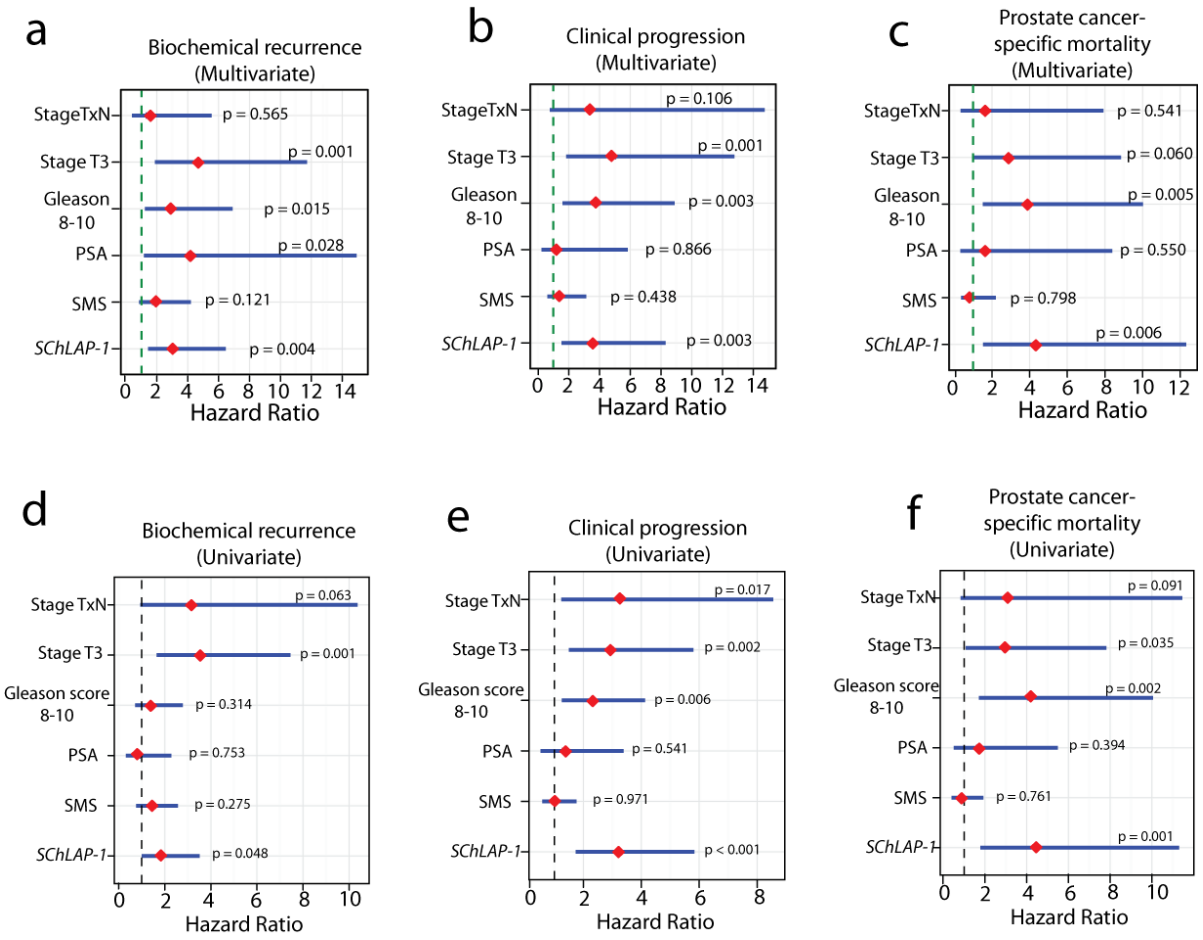

Supplementary Figure 7: *SChLAP1* expression is an independent predictor of patient clinical parameters. **(a-f)** Multivariate and univariate analyses for *SChLAP1* and disease outcomes. **(a-c)** Multivariate survival analyses demonstrate that *SChLAP1* is an independent predictor of prostate cancer biochemical recurrence (**a**), clinical progression (**b**), and prostate cancer-specific mortality (**c**) following radical prostatectomy. (**d-f**) Univariate survival analyses for *SChLAP1* for biochemical recurrence (**d**), clinical progression (**e**), and prostate cancer-specific mortality (**f**) as in (**a-c**). For these analyses, clinical significance was adjusted for confounding adjuvant

treatment, and Gleason score was dichotomized between those samples ≤7 ≥8. Red diamonds indicate the median hazard ratio for each factor and blue lines indicate the 95% confidence interval.

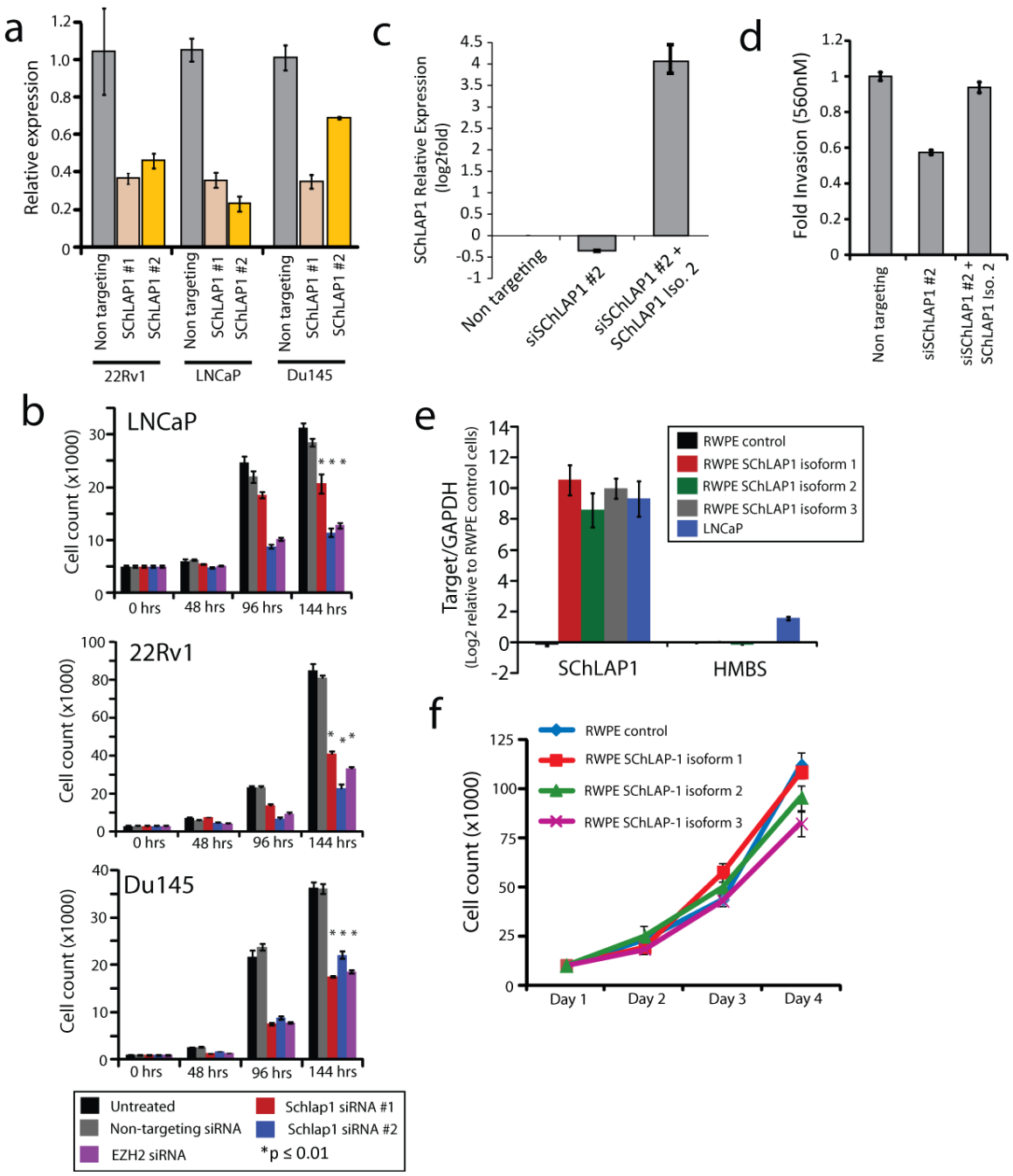

Supplementary Figure 8: *In vitro* knockdown and overexpression of *SChLAP1*. (a) 22Rv1, LNCaP, and Du145 cells were treated with siRNAs against *SChLAP1*. qPCR indicates relative knockdown efficiency in these cell lines. Error bars represent S.E.M. **(b)** Cell proliferation assays for LNCaP, 22Rv1, and Du145 treated with *SChLAP1*

siRNAs or non-targeting negative controls. *EZH2* siRNA serves as a positive control. Error bars indicate S.E.M. An asterisk (*) indicates $p < 0.05$ by Student's t-test. Error bars represent S.E.M. **(c)** Expression of *SChLAP1* in 22Rv1 cells treated with non-targeting, siRNA #2 for *SChLAP1*, or siRNA #2 with exogenous overexpression of *SChLAP1* isoform 2. **(d)** Boyden chamber invasion assay data for 22Rv1 cells treated with non-targeting, siRNA #2 for *SChLAP1*, or siRNA #2 with exogenous overexpression of *SChLAP1* isoform 2. Data are represented as absorbance at 560nM. Error bars represent S.E.M. **(e)** Overexpression of *SChLAP1* isoforms 1-3 in RWPE cells was confirmed using qPCR, which demonstrated that the overexpression resulted in comparable levels of *SChLAP1* transcript to LNCaP cells that express this gene endogenously. HMBS serves as a negative control. Error bars represent S.E.M. **(f)** Cell proliferation assays for RWPE cells overexpressing *SChLAP1* isoforms. No significant change in cell proliferation is observed. Error bars represent S.E.M.

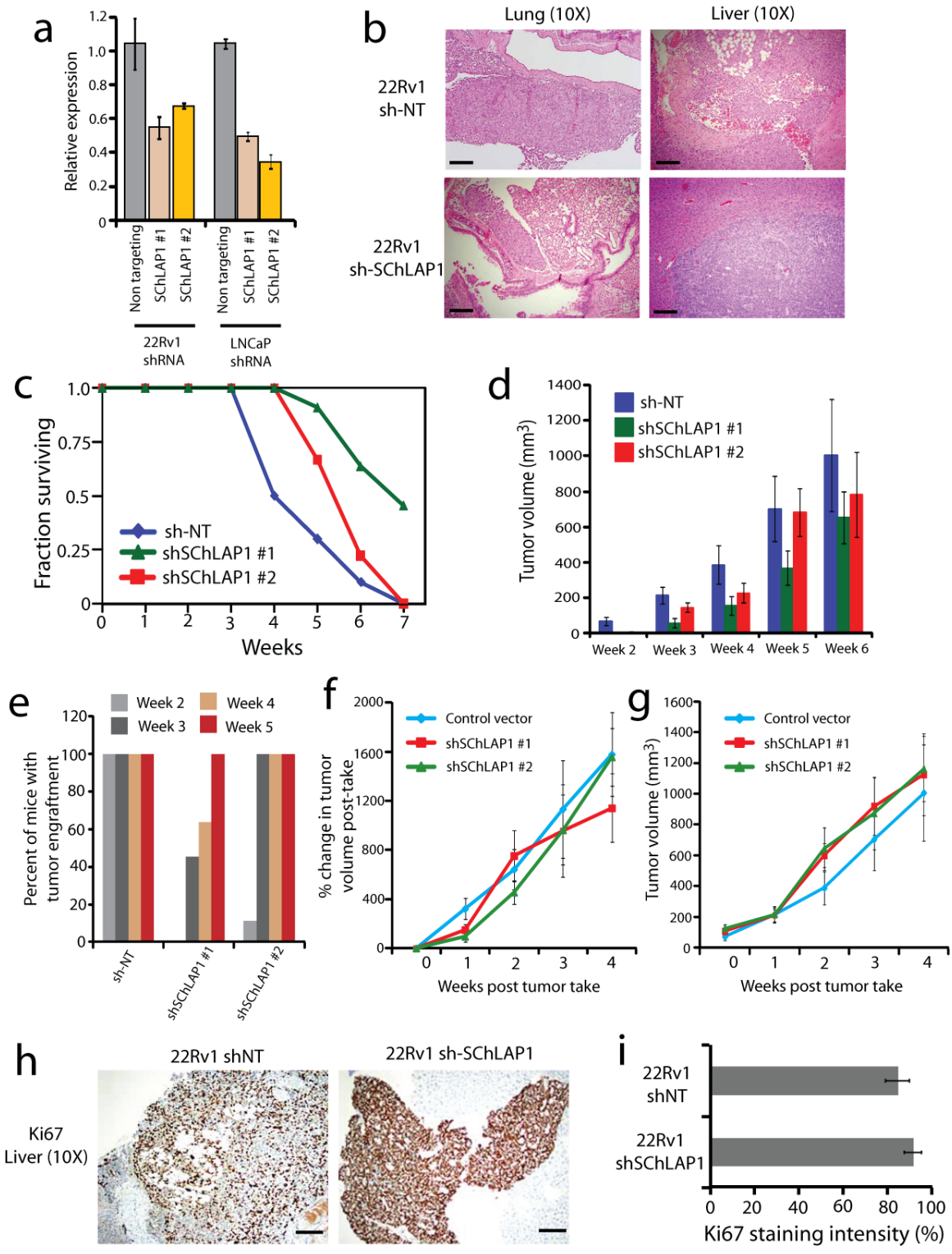

Supplementary Figure 9: Knockdown of *SChLAP1* delays tumor engraftment but not tumor growth kinetics. **(a)** Knockdown efficiencies for the shRNA knockdown of *SChLAP1* in LNCAP and 22Rv1 cells. Error bars indicate S.E.M. **(b)** Histolopathology

of murine tumors formed by intracardiac injection of 22Rv1 shNT or 22Rv1 sh-*SChLAP1* cells. Images are taken from the lungs and livers or mice with tumors. Slides are stained with H&E. **(c)** The fraction of mice surviving following subcutaneous injection of the 22Rv1 cell lines. This plot represents tumor-specific death of mice sacrificed when the tumor volume reached the maximum allowable volume. **(d)** 22Rv1 cells infected with lentivirus for shNT, sh-*SChLAP1* #1, and sh-*SChLAP1* #2 were injected subcutaneously in mouse flanks and tumor growth was monitored by caliper measurements. N = 10 mice for shNT cells, n = 12 mice for sh-*SChLAP1* #1 cells, n = 9 mice for sh-*SChLAP1* #2 cells. Absolute tumor volume for 22Rv1 shNT, sh-*SChLAP1* #1 and sh-*SChLAP1* #2 cells. Errors bars represent S.E.M. **(e)** Percent of mice with tumor engraftment over time. Knockdown of *SChLAP1* delays the onset of tumor engraftment. **(f)** The percent change in tumor volume per cell line normalized to the time of tumor engraftment. Errors bars represent S.E.M. **(g)** Tumor volume normalized to the time of tumor engraftment. Errors bars represent S.E.M. **(h)** Immunohistochemistry staining for Ki67 in 22Rv1 shNT and sh-*SChLAP1* liver metastases. **(i)** Summary of Ki67 tumor staining for 22Rv1 shNT and sh-*SChLAP1* murine tumors show significant difference in Ki67 staining intensity.

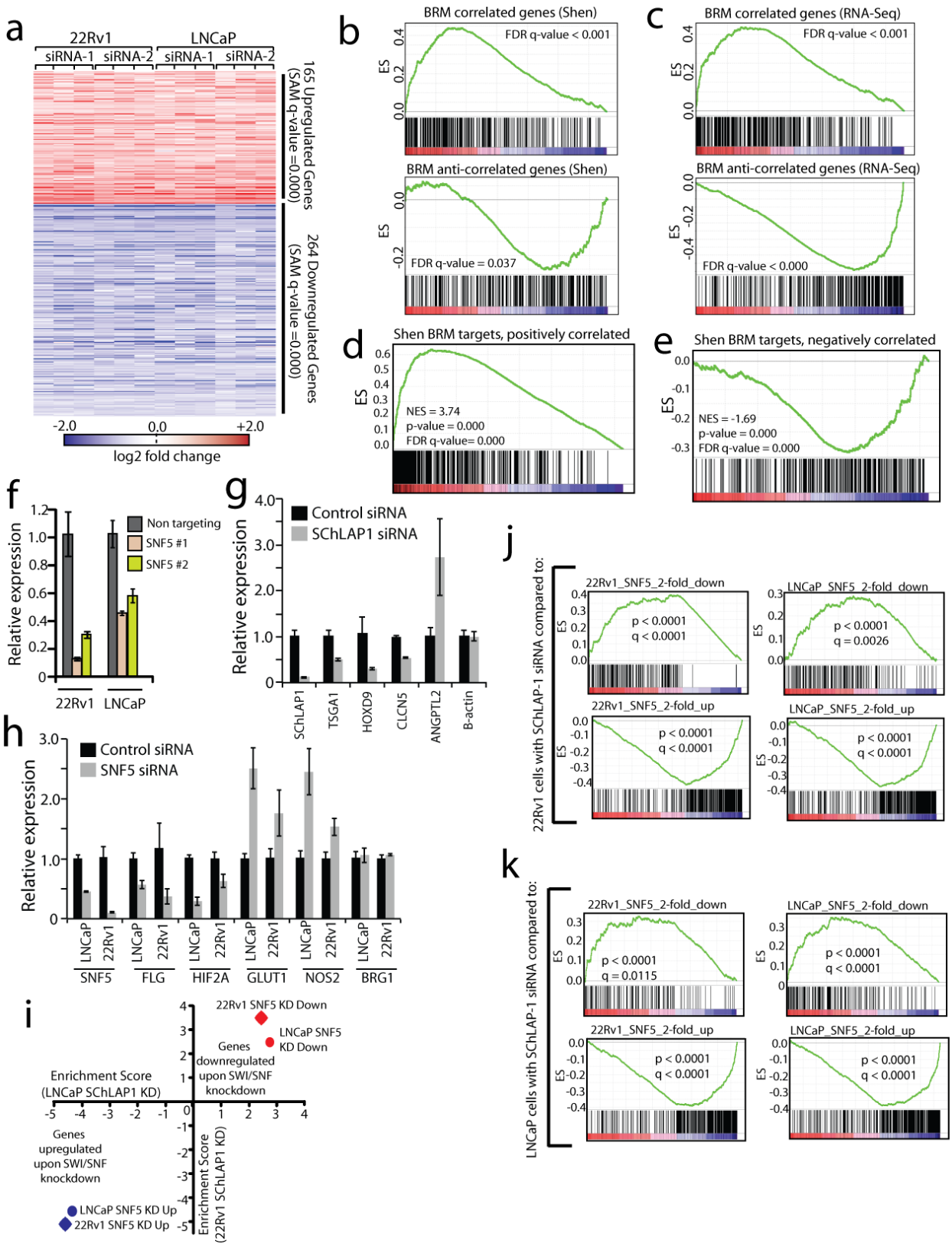
a
22Rv1
LNCaP
siRNA-1
siRNA-2
siRNA-1
siRNA-2
165 Upregulated Genes (SAM q-value =0.000)
264 Downregulated Genes (SAM q-value = 0.000)
-2.0
0.0
+2.0
log2 fold change
b
BRM correlated genes (Shen)
FDR q-value < 0.001
BRM anti-correlated genes (Shen)
FDR q-value = 0.037
c
BRM correlated genes (RNA-Seq)
FDR q-value < 0.001
BRM anti-correlated genes (RNA-Seq)
FDR q-value < 0.000
d
Shen BRM targets, positively correlated
NES = 3.74
p-value = 0.000
FDR q-value= 0.000
e
Shen BRM targets, negatively correlated
NES = -1.69
p-value = 0.000
FDR q-value = 0.000
f
Relative expression
Non targeting
SNF5 #1
SNF5 #2
22Rv1
LNCaP
g
Relative expression
Control siRNA
SChLAP1 siRNA
SChLAP1
TSGA1
HOXD9
CLCN5
ANGPTL2
B-actin
h
Relative expression
Control siRNA
SNF5 siRNA
LNCaP
22Rv1
SNF5
FLG
HIF2A
GLUT1
NOS2
BRG1
i
22Rv1 SNF5 KD Down
LNCaP SNF5 KD Down
Genes downregulated upon SWI/SNF knockdown
Enrichment Score (LNCaP SChLAP1 KD)
Genes upregulated upon SWI/SNF knockdown
LNCaP SNF5 KD Up
22Rv1 SNF5 KD Up
Enrichment Score (22Rv1 SChLAP1 KD)
j
22Rv1 cells with SChLAP-1 siRNA compared to:
22Rv1_SNF5_2-fold_down
p < 0.0001
q < 0.0001
LNCaP_SNF5_2-fold_down
p < 0.0001
q = 0.0026
22Rv1_SNF5_2-fold_up
p < 0.0001
q < 0.0001
LNCaP_SNF5_2-fold_up
p < 0.0001
q < 0.0001
k
LNCaP cells with SChLAP-1 siRNA compared to:
22Rv1_SNF5_2-fold_down
p < 0.0001
q = 0.0115
LNCaP_SNF5_2-fold_down
p < 0.0001
q < 0.0001
22Rv1_SNF5_2-fold_up
p < 0.0001
q < 0.0001
LNCaP_SNF5_2-fold_up
p < 0.0001
q < 0.0001

Supplementary Figure 10: *SChLAP1* and the SWI/SNF complex regulate gene expression in an opposing manner. (a) Transcriptome profiling following *SChLAP1* knockdown *in vitro*. Differentially expressed genes were determined by SAM analysis and represented as a heatmap. (**b-c**) Gene set enrichment analysis (GSEA) of LNCaP and 22Rv1 cells treated with *SChLAP1* siRNAs. GSEA results indicate that *SChLAP1* knockdown results are inversely correlated with SWI/SNF-associated genes using data from Shen *et al.* **(b)** or using RNA-seq data **(c)**. **(d)** Comparison of positively correlated BRM-associated gene signatures in prostate cancer. The BRM-derived signature from RNA-seq samples was compared to the Shen et al. signature by GSEA. A highly significant overlap between the signatures is observed. **(e)** Comparison of negatively correlated BRM-associated gene signatures in prostate cancer. The BRM-derived signature from RNA-seq samples was compared to the Shen et al. signature by GSEA. A highly significant overlap between the signatures is observed. **(f)** Knockdown efficiency of *SNF5* siRNAs in 22Rv1 and LNCaP. Error bars represent S.E.M. (**g**) Gene expression changes nominated by microarray analysis of SChLAP1 knockdown samples are confirmed by qPCR in LNCaP cells treated with SChLAP1 siRNA #1. B-actin serves as a control. **(h)** Gene expression changes nominated by microarray analysis of SNF5 knockdown samples are confirmed by qPCR in LNCaP and 22Rv1 cells. BRG1 serves as a control. **(i)** GSEA analysis of *SChLAP1* and *SNF5* knockdowns. Across two cell lines (LNCaP and 22Rv1), *SChLAP1* knockdown had the opposite effect on gene expression as knockdown of *SNF5*. Here, a positive GSEA normalized enrichment score (NES) indicates genes up-regulated upon *SChLAP1* knockdown, and a negative GSEA NES indicates genes down-regulated upon *SChLAP1* knockdown. **(j)** GSEA results from

comparisons of *SChLAP1* and *SNF5* knockdown in 22Rv1 cells. *SChLAP1* was knocked-down using siRNAs in 22Rv1 cells. Gene expression changes were compared using GSEA to expression changes observed using *SNF5* siRNAs in LNCaP or 22Rv1 cells. The enrichment plots of these comparisons are shown. **(k)** GSEA results from comparisons of *SChLAP1* and *SNF5* knockdown in LNCaP cells. *SChLAP1* was knocked-down using siRNAs in LNCaP cells. Gene expression changes were compared using GSEA to expression changes observed using *SNF5* siRNAs in LNCaP or 22Rv1 cells. The enrichment plots of these comparisons are shown.

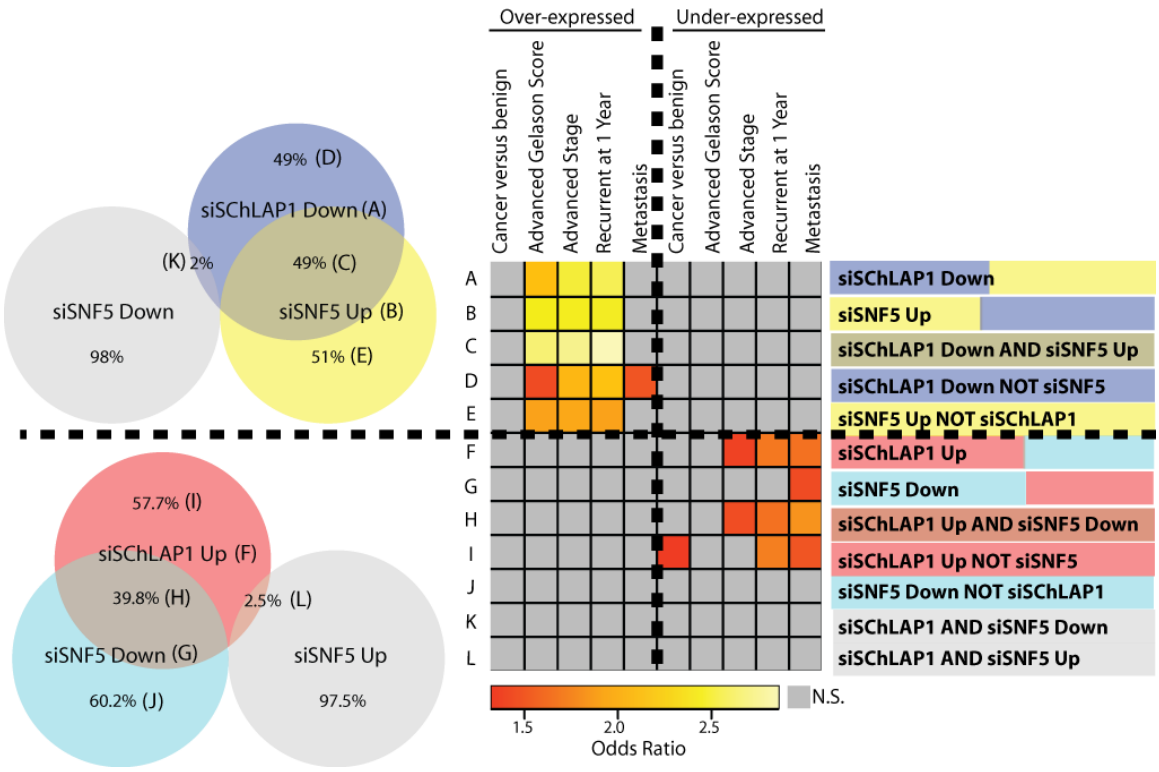

Supplementary Figure 11: *SChLAP1* and *SNF5* co-regulate genes associated with prostate cancer aggressiveness. The top 10% of up- or down-regulated genes for SNF5-knockdown or SChLAP1-knockdown microarrays in 22Rv1 and LNCaP were intersected to generate an overlapping gene signature for these knockdown experiments. This signature was analyzed for overlap with the Taylor Prostate 3 Oncomine Concept[8] for disease aggressiveness. *Left,* Venn diagrams demonstrating overlap of SChLAP1 and SNF5-knockdown experiments. *Right,* a heatmap visualization showing statistical ($q < 0.05$) overlap of gene signatures from the SNF5 and SChLAP1 knockdowns with prostate cancer aggressiveness concepts from Oncomine. Odds ratios from the comparisons with q-values <0.05 are shown. One-sided Fisher's exact tests were used for significance.

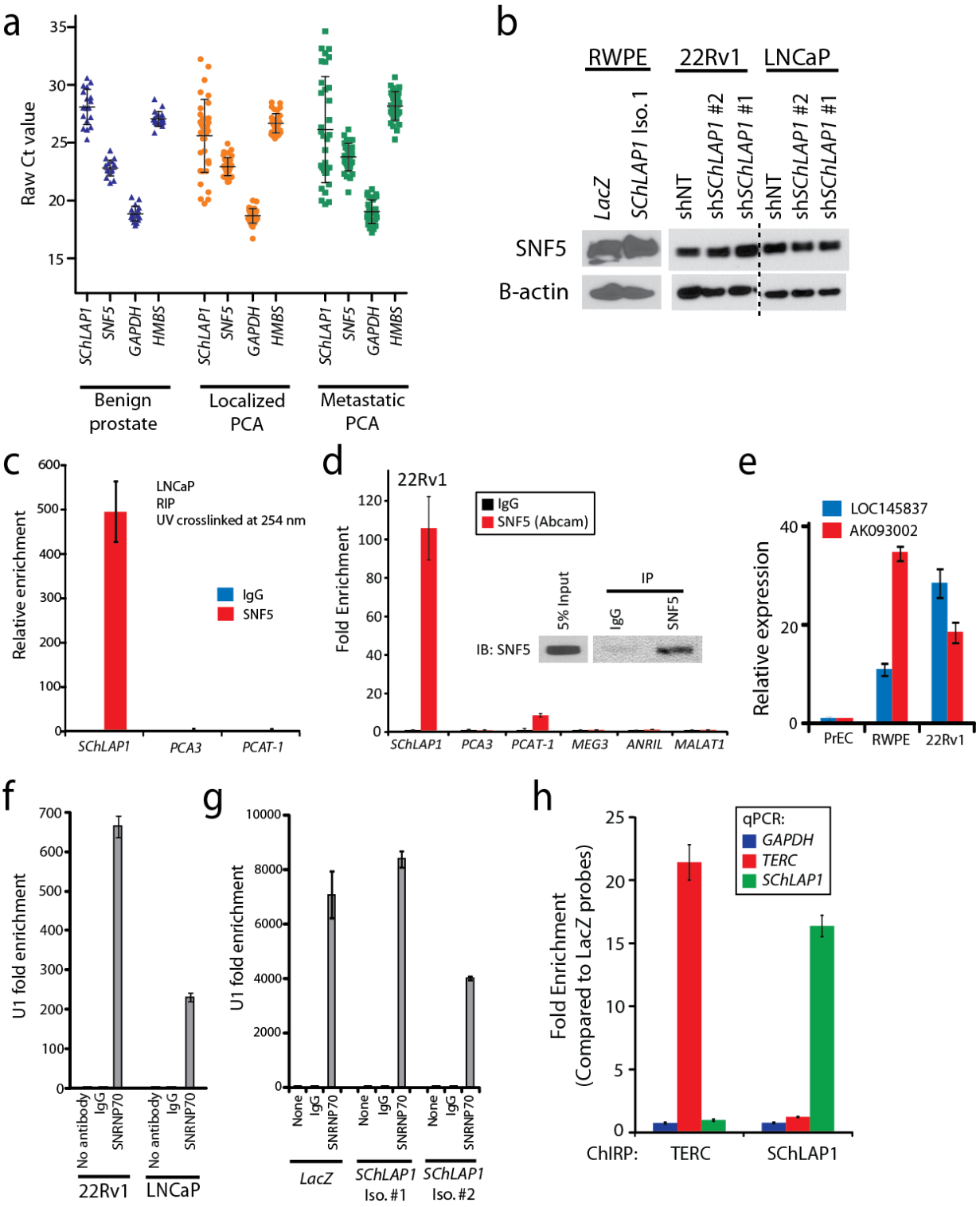

Supplementary Figure 12: *SChLAP1* and SNF5 expression level and RNA-protein binding of *SChLAP1* with SNF5. (a) Relative abundance of SChLAP1 compared to the SWI/SNF complex in human prostate tissues. qPCR cycle threshold (Ct) values for

SChLAP1, SNF5, GAPDH, and HMBS are shown. SChLAP1-positive samples display Ct values in the low 20s, which is consistent with the abundance of SNF5. **(b)** Western blot analysis of SNF5 protein abundance in prostate cancer cells either overexpressing *SChLAP1* (RWPE) or with stable knockdown of *SChLAP1* (22Rv1, LNCaP). **(c)** SChLAP1 binding to SNF5 protein by UV-crosslinked RIP assays using UV at 254nM. **(d)** Co-immunoprecipitation of SChLAP1 with SNF5 using a second independent antibody. The inset Western blot confirms efficiency of the SNF5 immunoprecipitation. **(e)** Expression of AK093002 and LOC145837 in prostate cell lines. qPCR data were normalized to the average of *GAPDH* + *B-actin* and compared to PREC primary non-immortalized prostate cells. Error bars indicate S.E.M. Expression of these genes in RWPE is comparable to their expression in 22Rv1. **(f)** RNA-IP experiments for SNRNP70 in LNCaP and 22Rv1 shows binding of SNRNP70 to the U1 ncRNA, indicating specificity of the RNA-IP experiments. Error bars indicate S.E.M. **(g)** Control SNRNP70 experiments in the RWPE-*SChLAP1* overexpression models. Enrichment of U1 is shown as a control for SNRNP70 IP experiments. **(h)** Pulldown of SChLAP1 RNA. RWPE-SChLAP1 isoform #1 cells were treated with biotinylated SChLAP1, TERC or LacZ RNA probes according to the ChIRP protocol[9]. Quantification of RNA pulldown efficiency by qPCR is shown. Error bars indicate S.E.M.

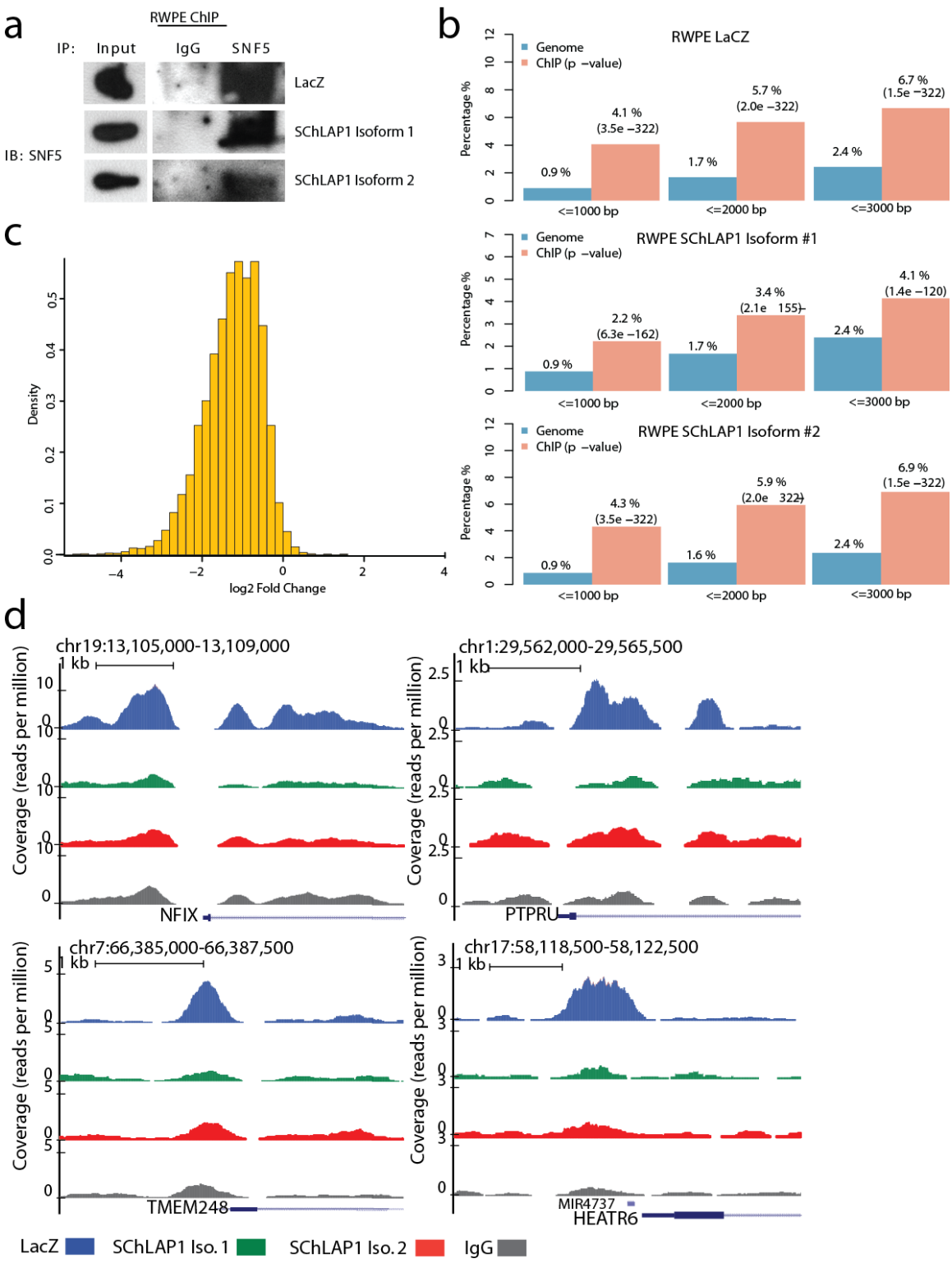
a
RWPE ChIP
IP: Input IgG SNF5
LacZ
SChLAP1 Isoform 1
SChLAP1 Isoform 2
IB: SNF5
b
RWPE LaCZ
Genome
ChIP (p −value)
Percentage %
0.9 %
4.1 %
(3.5e −322)
1.7 %
5.7 %
(2.0e −322)
2.4 %
6.7 %
(1.5e −322)
<=1000 bp
<=2000 bp
<=3000 bp
RWPE SChLAP1 Isoform #1
2.2 %
(6.3e −162)
3.4 %
(2.1e 155)
4.1 %
(1.4e −120)
RWPE SChLAP1 Isoform #2
4.3 %
(3.5e −322)
5.9 %
(2.0e 322)
6.9 %
(1.5e −322)
c
Density
log2 Fold Change
d
chr19:13,105,000-13,109,000
chr1:29,562,000-29,565,500
chr7:66,385,000-66,387,500
chr17:58,118,500-58,122,500
1 kb
Coverage (reads per million)
NFIX
PTPRU
TMEM248
MIR4737
HEATR6
LacZ
SChLAP1 Iso. 1
SChLAP1 Iso. 2
IgG

Supplementary Figure 13: *SChLAP1* expressed disrupts genomic binding of SNF5. **(a)** ChIP for SNF5 protein followed by Western blot. **(b)** Bar plots showing enrichment for SNF5 ChIP-Seq reads at RefSeq gene promoters across the RWPE-*LacZ*, RWPE-*SChLAP1*-Isoform-1 and RWPE-*SChLAP1*-Isoform-2 samples. Blue bars indicate percentage of genomic DNA and red bars indicate percentage of all ChIP-Seq reads in each sample along with the p-value corresponding to the statistical significance of the difference between the blue and red bars. The CEAS software was used to generate these plots and compute the enrichment. **(c)** Histogram showing the relative $\log_2$ fold-change between RWPE-*LacZ* and RWPE-*SChLAP1* (average of both isoforms) coverage across 6,235 genome-wide peaks. **(d)** Example ChIP-Seq binding sites for SNF5 on gene promoters. SNF5 binding is higher at gene promoters in RWPE-*LacZ* cells and decreased upon *SChLAP1* overexpression.

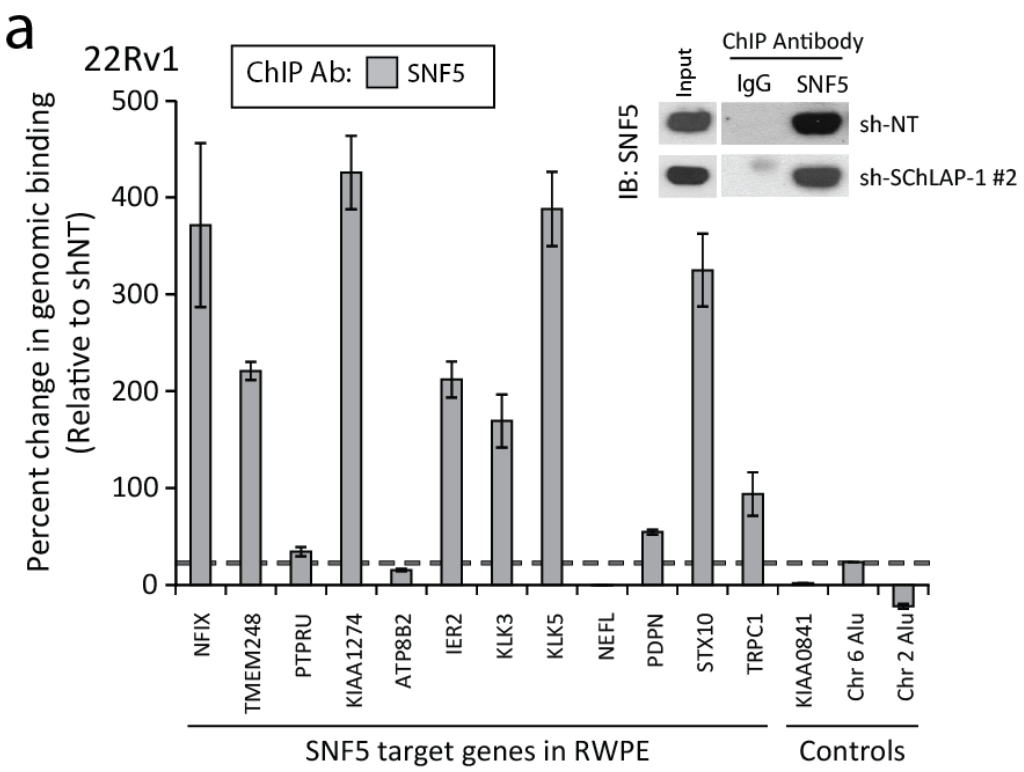
a
22Rv1
ChIP Ab: SNF5
Percent change in genomic binding
(Relative to shNT)
500
400
300
200
100
0
ChIP Antibody
Input
IgG
SNF5
IB: SNF5
sh-NT
sh-SChLAP-1 #2
NFIX
TMEM248
PTPRU
KIAA1274
ATP8B2
IER2
KLK3
KLK5
NEFL
PDPN
STX10
TRPC1
KIAA0841
Chr 6 Alu
Chr 2 Alu
SNF5 target genes in RWPE
Controls

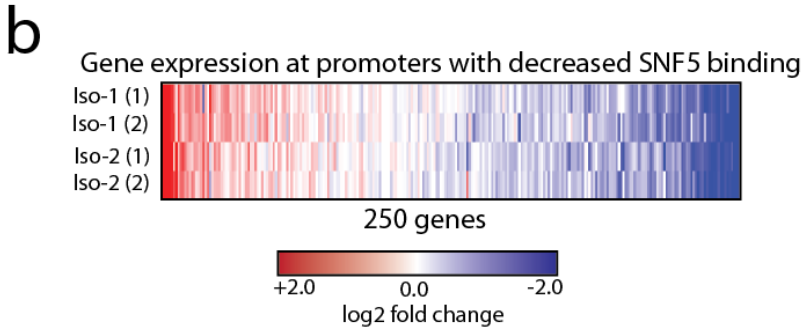
b
Gene expression at promoters with decreased SNF5 binding
Iso-1 (1)
Iso-1 (2)
Iso-2 (1)
Iso-2 (2)
250 genes
+2.0
0.0
-2.0
log2 fold change

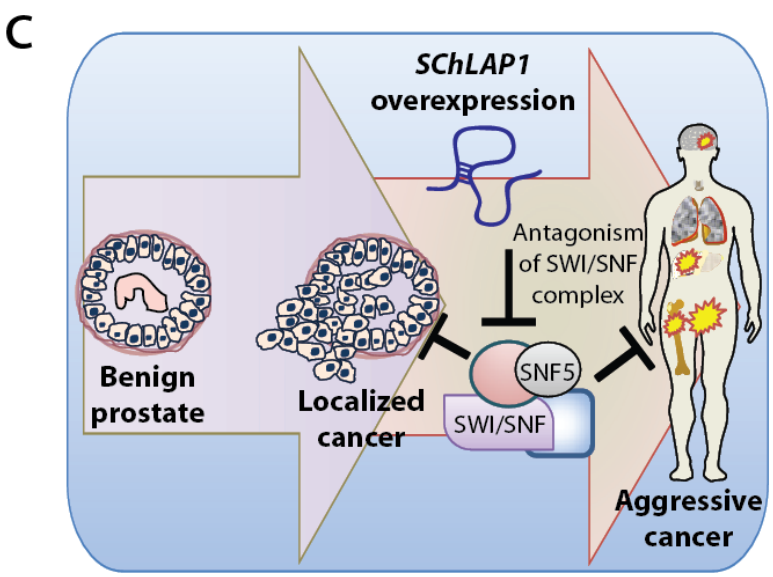
c
SChLAP1
overexpression
Antagonism
of SWI/SNF
complex
SNF5
SWI/SNF
Benign
prostate
Localized
cancer
Aggressive
cancer

Supplementary Figure 14: Confirmation of SNF5 target genes by ChIP.

(a) ChIP for SNF5 in 22Rv1 shNT and 22Rv1 sh-SChLAP1 #2. ChIP-PCR for 9 of 12 target genes of SNF5 in RWPE demonstrates an increase in SNF5 binding upon SChLAP1 knockdown. KIAA0841, Chr6 Alu, and Chr 2 Alu serve as negative controls. Data are represented as percent change in genomic binding relative to shNT after being normalized to IgG controls. The inset western blot indicates immunoprecipitation efficiency for SNF5. **(b)** Heatmap showing the showing the gene expression of RWPE-*SChLAP1* cells (Isoform 1 is labeled as Iso-1 and Isoform 2 is labeled as Iso-2) across 250 genes that exhibited a >2-fold decrease in SNF5 binding upon *SChLAP1* overexpression. Gene expression is shown as $\log_2$ fold-change relative to RWPE-*LacZ*. **(c)** A schematic of SChLAP1 function in prostate cancer.

Tables

Supplementary Table 1 (separate file): RNA-Seq sample information
Supplementary Table 2 (separate file): U-M sample clinical information
Supplementary Table 3 (separate file): Gene correlation signature
Supplementary Table 4 (separate file): Mayo Clinic sample information
Supplementary Table 5 (separate file): Microarray knockdown results
Supplementary Table 6 (separate file): ChIP-Seq results
Supplementary Table 7 (separate file): Primers used
Supplementary Table 8 (separate file): ChIRP probe sequences

Supplementary References

1. Simmons, M.N., Stephenson, A.J. & Klein, E.A. Natural history of biochemical recurrence after radical prostatectomy: risk assessment for secondary therapy. *Eur Urol* **51**, 1175-84 (2007).
2. Boorjian, S.A. *et al.* Long-term risk of clinical progression after biochemical recurrence following radical prostatectomy: the impact of time from surgery to recurrence. *Eur Urol* **59**, 893-9 (2011).
3. Tomlins, S.A. *et al.* The role of SPINK1 in ETS rearrangement-negative prostate cancers. *Cancer Cell* **13**, 519-28 (2008).
4. Kim, J.H. *et al.* Integrative analysis of genomic aberrations associated with prostate cancer progression. *Cancer Res* **67**, 8229-39 (2007).
5. Han, B. *et al.* Fluorescence in situ hybridization study shows association of PTEN deletion with ERG rearrangement during prostate cancer progression. *Mod Pathol* **22**, 1083-93 (2009).
6. Setlur, S.R. *et al.* Estrogen-dependent signaling in a molecularly distinct subclass of aggressive prostate cancer. *J Natl Cancer Inst* **100**, 815-25 (2008).
7. Glinsky, G.V., Glinskii, A.B., Stephenson, A.J., Hoffman, R.M. & Gerald, W.L. Gene expression profiling predicts clinical outcome of prostate cancer. *J Clin Invest* **113**, 913-23 (2004).
8. Taylor, B.S. *et al.* Integrative genomic profiling of human prostate cancer. *Cancer Cell* **18**, 11-22 (2010).
9. Chu, C., Qu, K., Zhong, F.L., Artandi, S.E. & Chang, H.Y. Genomic maps of long noncoding RNA occupancy reveal principles of RNA-chromatin interactions. *Mol Cell* **44**, 667-78 (2011).